CONTINUOUS NUMERICAL METHOD IN ANALYSIS OF AXIS-SYMMETRIC EXTRUSION PROBLEMS: NUMERICAL EXPERIMENTS AND APPLICATION

C. O. Izelu - C. A. Ebiogwu - F. F. Orumwense
Department of Mechanical Engineering, Faculty of Engineering, University of Benin, Benin City, Nigeria
izelu2003@yahoo.com- chika_ebiogwu@yahoo.com– orumwense@yahoo.com

Abstract
The CNM approach to solutions of extrusion problems has been formulated in Izelu et al [15]. The Procedure and results of numerical experiments performed, with some axis-symmetric profiled dies are reported. The results showed that the method is simple and straightforward in its formulation and implementation with the digital computer, and involves less complex mathematical details and minimal geometrical restrictions. They also showed that it is capable of providing, with dense numerical output, direct and complete solution of the metal flow problems in axis-symmetric extrusion together with full predictions of the process performance in any given set of steady-state extrusion conditions. The predicted effects of the interface friction factor and extrusion ratio on die performance are quite in agreement with predictions of other methods.

Keywords: Compressive plastic deformation process, axis-symmetric steady-state extrusion, cylindrical co-ordinate region, grid-lines, grid-points, off grid-points, collocation method, and profiled die.

Notations

S	Plastic Flow Zone or Region
r, θ, z	Cylindrical Co-ordinates of Region, S
v_r, v_θ, v_z	Velocity Components in Cylindrical Co-ordinates
$\varepsilon_r, \varepsilon_\theta, \varepsilon_z$	Strain-Rate Components in Cylindrical Co-ordinates
$\gamma_{rz}, \gamma_{\theta r}, \gamma_{\theta z},$	Shear Strain-Rate Components in Cylindrical Co-ordinates
$\sigma_r, \sigma_\theta, \sigma_z$	Stress Components in Cylindrical Co-ordinates
$\tau_{rz}, \tau_{\theta r}, \tau_{\theta z}$	Shear Stress Components in Cylindrical Co-ordinates
δ_{ij}	Kroneker Delta: $\delta = 1$, for $i \neq j$; $\delta = 0$, for $i = j$
$v, \varepsilon, e, \sigma$	Effective Velocity, Strain-Rate, Strain and Stress, Respectively
p	Hydrostatic Pressure
λ	Plastic Compliance of Materials
C	Material Constant (C is the Yield or Flow Stress of Materials)
k	Yield Shear Stress of Material
n, m	Strain Hardening Exponent, and Strain-Rate Sensitivity Factor, Respectively
T	Absolute Billet Temperature
ϕ	Flow Field or Stream Function
N,P	Order of the Approximating Function, and Number of Grid or Stream Lines, Respectively
$C_{j,s}$	Flow Field or Stream Function Coefficients
$V_{j,s}$	Velocity Field Function Coefficients
$\Omega_{j,s}$	Strain-Rate Field Function Coefficients
$\Pi_{j,s}$	Shear Strain-Rate Field Function Coefficients
v_1, v_2	Dimensionless Entrance and Exit Velocities of the Billet, Respectively
r_1, r_2	Dimensionless Entrance and Exit Radii of the Billet, Respectively
z_1, z_2	Axial Positions of the die at Entrance and Exit, Respectively
α	Semi-Angle of the Die
L	Dimensionless Axial Length of the Die

L_c, L_l	Dimensionless Axial Length of the Container and Die Land Respectively
R	Fractional Reduction of Area
R_e	Extrusion Ratio
σ_{fp}	Front Pull Stress
P_{he}, P_{fe}, P_{re},	Homogeneous or Ideal, Friction, and Redundant Components of the Actual Extrusion Pressure, Respectively
P_{ae}	Actual Extrusion Pressure
$P_{ds,}$ P_{db}	Die Surface, and Breaking Pressure, Respectively
P_c, P_l	Pressure Due to Container, and Land Friction, Respectively
η, ψ	Die Efficiency and Redundancy Factor, Respectively
m_f, m_s	Friction and Shear factor, respectively

Introduction

An investigation of a new numerical approach to the solution of metal forming problems has been undertaken, with its formulation and application in the study of the mechanics of axis-symmetric extrusion reported in Izelu et al, [15]. The formulation involved finding a power series approximate solution of the governing Biharmonic Partial Differential Field Equation (BPDFE), posed in the plastic cylindrical co-ordinate region. In order to achieve this major purpose, the field equation was mathematically decomposed into an Ordinary Differential Equation (ODE) by means of the Centred Finite-divided Difference Equations (CFDE). When the Dirichlet boundary conditions were applied, a coupled system of boundary value problem of the type found in the axis-symmetric extrusion process was produced. Solving this system, with the collocation method, yielded a set of linear algebraic equations in coefficients of the assumed flow functions defined as polynomial functions. The knowledge of these unknown flow function coefficients, through solution of the resulting set of linear algebraic equations, was necessary for the evaluation of the grid-line flow functions, and the formulated field equations for the flow variables of extrusion. Expressions, which demonstrate how the extrusion and die pressure, and the process performance might be predicted from the field data, were also presented in Izelu et al [15].

The foundation works employed in the axis symmetric formulation of the CNM approach include Chakrabarty [7]; Gurney and De pierre [9]; Hosford and Caddell [10]; Johnson and Kudo [11]; Lee and Male [12]; Lee and Patel [13]; and Zimerman and Avitzor [16]. More recent literatures used in the formulation of the CNM approach include Badaru [1]; Badaru and Onumanyi [2]; Badaru and Oyebo [3]; Badaru and Quoye [4]; Badaru and Yusuf [5]; Blazynski [6]; Chapra and Canale [8]; and Mielnik [14]. The notations used in the formulation are given above.

In the course of development of any numerical technique, numerical data are often required to be able to certify and accord the technique with the privilege of being adopted as an analytical tool. The essence of a numerical tool is not only in the possibility of obtaining numerical data that explains some of the physical phenomena, but also, in the use of these data in the determination of its efficacy and utility. Most often, numerical experiments are designed in order to obtain numerical data with the aid of digital computer. In this work, the flow field data, velocity field data, strain-rate field data, strain field data, hydrostatic pressure field data and the stress field data are the major set of numerical data of interest. The mean values of these data constitute the flow variables of extrusion. In any process design and analysis, these are required to be able to estimate the extrusion pressure, die pressures and the die performance parameters, which, in turn, constitute the die or process performance data. While the press capacity requirement is determined from knowledge of the extrusion pressure, the strength capability of the die materials is assessed from knowledge of the die pressures. On the other hand, the ability of the die to produce products with sound surface and internal structure is

assessed from knowledge of the die performance parameters. The study of relationships existing amongst the various extrusion variables often leads to the determination of the optimum extrusion conditions.

The purpose of this paper, therefore, is to document the adopted computational procedure and implementation, and the results of the numerical experiments performed with some profiled dies in order to test the efficacy of the method and ascertain its utility.

Computational Procedure and Implementation

The various steps involved in obtaining the numerical data, with the aid of the digital computer, are detailed as follows:

Step 1: Select a die and its profile equation, r = r (z). Decide on the shape of the shear boundaries, B_1 and B_2, at the die entrance and exit, respectively. Note that the axial and friction boundaries, B_0 and B_3, conform to the shape of the die axis and profile, respectively.

Step 2: Select any combination of P and N.

Step 3: Input the values for r_1 and r_2; z_1 and z_2; v_1; and m $_f$. Then, compute $L = z_1-z_2$; $R = (r_1^2-r_2^2)/r_1^2$; $R_e = r_1^2/r_2^2$; $a = \tan^{-1}\{(r_1-r_2)/L\}$; and $v_2 = (r_1^2/r_2^2)\, v_1$. Establish the grid-line values of B_1 and B_2, and the grid-point values of B_0 and B_3.

Step 4: Set up and evaluate the elements of the matrix, $r_s = r_s(z)$, for the grid-point values, $z = z_i$, on the interval $0 \leq z \leq L$.

Step 5: Set up and evaluate the elements of the geometric matrix, $r_s = r_s(z)$, for the grid-point values, $z = L$; $z_i = \{1/5, 2/5, 3/5, 4/5\}L$; and $z_k = \{1/10, 3/10, 5/10, 7/10\}L$.

Step 6: Set up and evaluate elements of the coefficient vectors, q_e, $e = \{1, \ldots, 9\}$, of the ODE

Step 7: Set up and evaluate the elements of the block matrices A_e, $e = \{1, 2, 3\}$; B_e, $e = \{1, 2\}$; U_e, $e = \{1, 2\}$, and O. Then assemble them into the main matrix, [G].

Step 8: Set up and evaluate the elements of the vector, {D}.

Step 9: Set up the matrix equation, $[G]\{C\} = \{D\}$, solve for {C}, and then, evaluate the flow function, $\phi_{N,s} = \phi_{N,s}(z)$, for the grid-point values, $z = z_i$, on the interval $0 \leq z \leq L$.

Step 10: Set up and evaluate the elements of the vectors, $V_{rj,s}$ and $V_{zj,s}$. Then, evaluate the velocity functions, $v_{rN,s} = v_{rN,s}(z)$; $v_{zN,s} = v_{zN,s}(z)$; $v_{N,s} = v_{N,s}(z)$; and the direction of $v_{N,s}$, $\varphi_{N,s} = \varphi_{N,s}(z)$, for the grid-point values, $z = z_i$, on the interval $0 \leq z \leq L$.

Step 11: Set up and evaluate the elements of the vectors, $\Omega_{rN,s}$, $\Omega_{\theta N,s}$, $\Omega_{zN,s}$, $(\Pi_{rzN,s})^{**}$, and $(\Pi_{rzN,s})^{*}$. Then, evaluate the strain-rate functions, $\varepsilon_{rN,s} = \varepsilon_{rN,s}(z)$; $\varepsilon_{\theta N,s}(z) = \varepsilon_{\theta N,s}(z)$; $\varepsilon_{zN,s} = \varepsilon_{zN,s}(z)$; $\gamma_{rzN,s} = \gamma_{rzN,s}(z)$; $\varepsilon_{N,s} = \varepsilon_{N,s}(z)$; and strain function, $e_{N,s} = e_{N,s}(z)$, for the grid-point values, $z = z_i$, on the interval $0 \leq z \leq L$.

Step 12: Obtain the CNM solution, $\{\chi\}$, of the hydrostatic pressure field equation reduced to the form, $[M]\{\chi\} = \{\delta\}$. Then, evaluate the hydrostatic pressure functions, $p_{N,s}/C = p_{N,s}(z)/C$, for the grid-point values, $z = z_i$, on the interval, $0 \leq z \leq L$, and obtain the mean hydrostatic pressure, p.

Step 13: Evaluate the stress functions, $\sigma_{rN,s} = \sigma_{rN,s}(z)$; $\sigma_{\theta N,s} = \sigma_{\theta N,s}(z)$; $\sigma_{zN,s} = \sigma_{zN,s}(z)$; $\iota_{rzN,s} = \iota_{rzN,s}(z)$ and $\sigma_{N,s} = \sigma_{N,s}(z)$, for the grid-point values, $z = z_i$, on the interval, $0 \leq z \leq L$.

Step 14: Obtain the values of the extrusion pressures, P_{he}/C, P_{fe}/C, P_{re}/C, and P_{ae}/C, including P_{ne}/C and P_{te}/C, for a specific problem; die performance parameters, η and ψ; and die pressures, P_{ds}/C, P_{db}/C, and P_{dc}/C.

Step 15: Output results, which may be numerical and/or graphical.

CNM solutions may be implemented with any of the standard mathematical software packages, such as MathCad, MatLab, and Mathematica; or spreadsheet programs, such as Microsoft Excel, Lotus 1 2 3, and Corel Quattro Pro. However, Microsoft Excel 97 is used in the present situation, as a matter of convenience and availability, and with little stress, as less complex mathematical details are involved.

Results and Discussion

Numerical experiments were performed with the axis-symmetric extrusion dies, such as conical die (A), and the curved dies of the convex profile (B), concave profile (C) and the sigmoidal profile (D). The convex profiled dies, which were considered include the parabolic die (B-A), hyperbolic die (B-B) and the convex circular-arc die (B-C). The concave profiled dies, which were considered include the sine-curved die (C-A), exponential die (C-B), elliptic die (C-C), and the concave circular-arc die (C-D), whereas, cosine-curved die (D) was the only sigmoidal profiled die studied. These are revolutions of the profile equations given in the appendix.

Table 1: Possible Combinations of P and N and Size of the Geometric

Case	**A**			**B**			**C**		
	P	N	(P-1)N	P	N	(P-1)N	P	N	(P-1)N
1	5	4	16	6	4	20	7	4	24
2	5	5	20	6	5	25	7	5	30
3	5	6	24	6	6	30	7	6	36
4	5	7	28	6	7	35	7	7	42
5	5	8	32	6	8	40	7	8	48
6	5	9	36	6	9	45	7	9	54
Case	**D**			**E**			**F**		
	P	N	(P-1)N	P	N	(P-1)N	P	N	(P-1)N
1	8	4	28	9	4	32	10	4	36
2	8	5	35	9	5	40	10	5	45
3	8	6	42	9	6	48	10	6	54
4	8	7	49	9	7	56	10	7	63
5	8	8	56	9	8	64	10	8	72
6	8	9	63	9	9	72	10	9	81

In order to compare results, the same basic dimensions were specified for these dies. That is, $r_1 = 2.0$; $r_2 = 1.0$; $z_1 = 1.0$; and $z_2 = 0.0$, but for the circular arc dies, $z_1 \approx 1.73$. These give rise to $R_e = 4.00$, $R = 0.75$, $L = 1.00$ (or ≈ 1.73, for circular-arc dies), and $\alpha = 45^0$. In each case, the die-material interface friction was assumed to be constant, and its value was set at $m_f = 0.0$, while the effects of temperature and time were assumed to be insignificant. That is, steady state, cold, and gradually loaded extrusion conditions, which may render temperature, and time invariant, are assumed. The shape of the flow or grid lines were assumed to be in conformity with the shape of the die profile, whereas, in order to further simplify the problems, those of the shear boundaries were assumed to be in conformity with the transverse lines. A constant ram velocity, $v_1 = 1.0$, was also specified.

Based on these conditions, the CNM solutions were obtained for the various combinations of P and N as summarised in Table 1. In each case of the extrusion problems solved, the preferred solutions were obtained by comparing the absolute errors ($E_a = |\phi_2 - \phi_1/|\phi_2$) in the order of increasing N of the flow functions for the given P of the grid lines. The combinations of P and N, which give the preferred solutions, together with the corresponding relative errors, E_r, and the resulting mean values of the flow function, ϕ, are given in Table 2. Accuracy was found to be dependent on the combinations of N and P, however no definite pattern was observed. Cases of no solution occurred with higher order combinations of N and P. This may be attributed to the data handling capability of the software used, and may be resolved through the use of software capable of handling higher order matrix sizes. Otherwise, the singularity of the matrices involved may be responsible as is indicated by their determinants, which could be approximated to zero.

Table 2: Summary of Preferred Solutions

S/No	Ref. Code		Case A P = 5 N = 4-9	Case B P = 6 N = 4-9	Case C P = 7 N = 4-9	Case D P = 8 N = 4-9	Case E P = 9 N = 4-9	Case F P = 10 N = 4-9	Preferre Solution
1	A	**F**	5.86	3.75	5.18	9.25	11.08	33.02	Case D2
		$\mathbf{E_a}$	0.15	0.03	0.05	0.01	0.08	1.05	
2	B-A	**F**	6.00	3.82	5.58	8.28	10.79	30.58	Case B6
		$\mathbf{E_a}$	0.18	0.02	0.05	0.05	0.12	1.05	
3	B-B	**F**	2.85	3.79	5.15	8.21	9.26	26.09	Case C3
		$\mathbf{E_a}$	0.03	0.05	0.01	0.01	0.15	0.84	
4	B-C	**F**	0.79	2.72	3.74	4.68	11.47	16.21	Case B4
		$\mathbf{E_a}$	0.88	0.00	0.01	0.05	0.19	0.31	
5	C-A	**F**	5.97	7.23	5.45	6.07	12.79	76.84	Case D3
		$\mathbf{E_a}$	0.13	0.19	0.16	0.03	0.17	0.93	
6	C-B	**F**	5.21	4.66	6.44	128.31	12.28	8.44	Case A2
		$\mathbf{E_a}$	0.00	0.02	0.09	0.87	0.25	0.20	
7	C-C	**F**	9.30	-3.57	3.35	5.92	-49.87	21.22	Case D2
		$\mathbf{E_a}$	0.12	1.13	0.09	0.05	0.44	1.41	
8	C-D	**F**	5.61	4.48	6.27	13.77	12.06	33.38	Case E3
		$\mathbf{E_a}$	0.03	0.02	0.90	0.05	0.00	0.22	
9	D	**F**	2.56	3.81	4.36	7.34	9.54	26.51	Case C3
		$\mathbf{E_a}$	0.10	0.04	0.00	0.01	0.11	1.53	

Table 3: Coefficients of the Grid-Line Stream or Flow Functions, $F_{N,s}$

$\{C_{j,s}\}$	0	1	2	3	4	5	6	7	8
1	0.00	-0.12	0.27	0.78	1.59	2.80	1.02	22.42	4.00
2	0.00	19.27	40.14	48.70	41.89	26.25	42.70	-162.00	0.00
3	0.00	-43.52	-93.08	-114.96	-99.92	-63.27	-143.60	547.87	0.00
4	0.00	38.91	83.21	99.61	82.76	63.83	249.02	-818.06	0.00
5	0.00	-13.29	-29.30	-32.03	-21.32	-14.35	-92.18	661.10	0.00

The flow function coefficients obtained from the preferred solutions were used in the evaluation of the flow variables, which in turn, were used in the evaluation of components of the extrusion pressure, die performance parameters, and the die pressures. Sample coefficients of the flow functions and grid-line flow fuctions are given in Table 3 and appendix, respectively. The flow field data are too numerous to be documented here. However, only few of those obtained for the conical die are presented as shown in Figs 4 to 8 as varying with respect to the axial and radial positions.

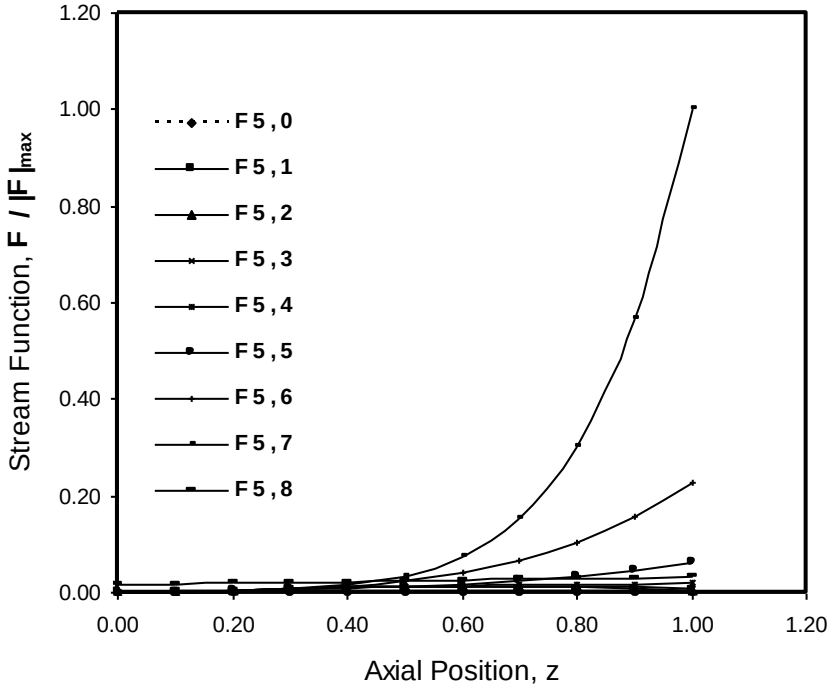

Figure 4(a): Normalised Flow Field (P = 8, N = 5, V1 = 1.0, R = 0.75, L = 1.0, m = 0.0)

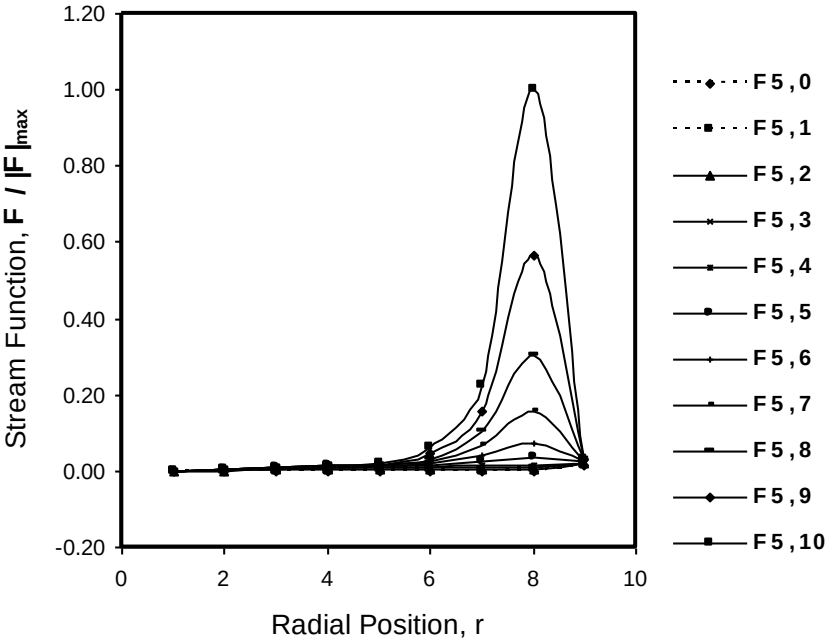

Figure 4(b): Normalised Flow Field (P = 8, N = 5, v_1 = 1.0, R = 0.75, L = 1.0, m = 0.0)

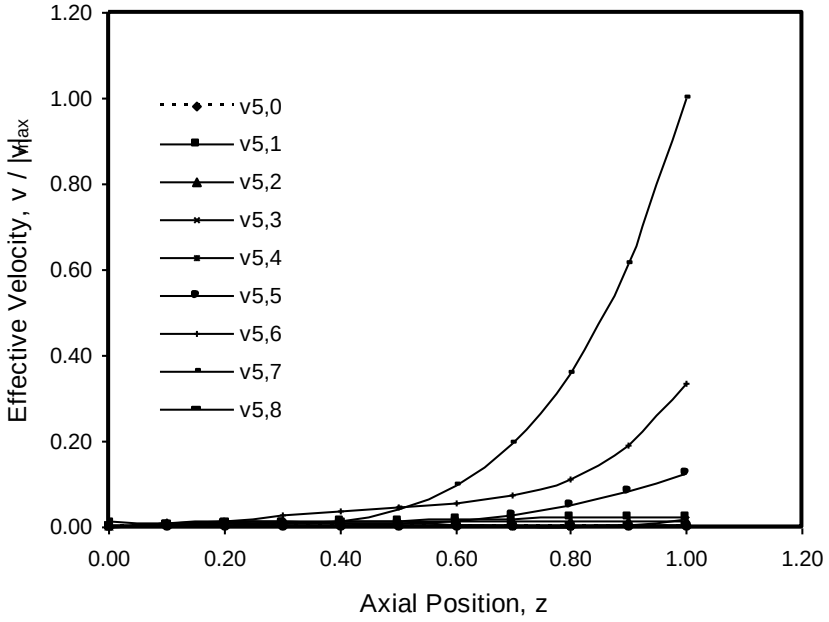

Figure 5(a): Normalised Velocity Field (P = 8, N = 5, V1 = 1.0, R = 0.75, L = 1.0, m = 0.0)

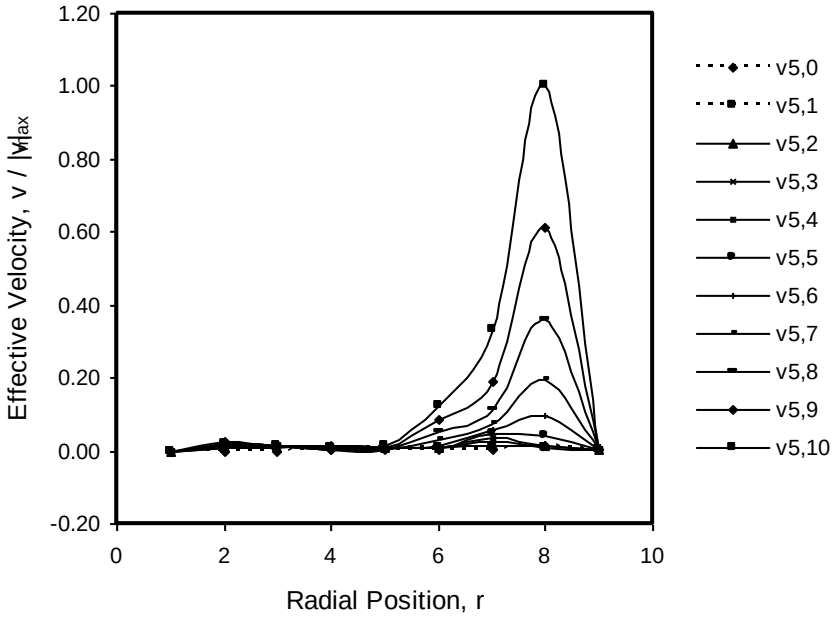

Figure 5(b): Normalised Velocity Field (P = 8, N = 5, V1 = 1.0, R = 0.75, L = 1.0, m = 0.0)

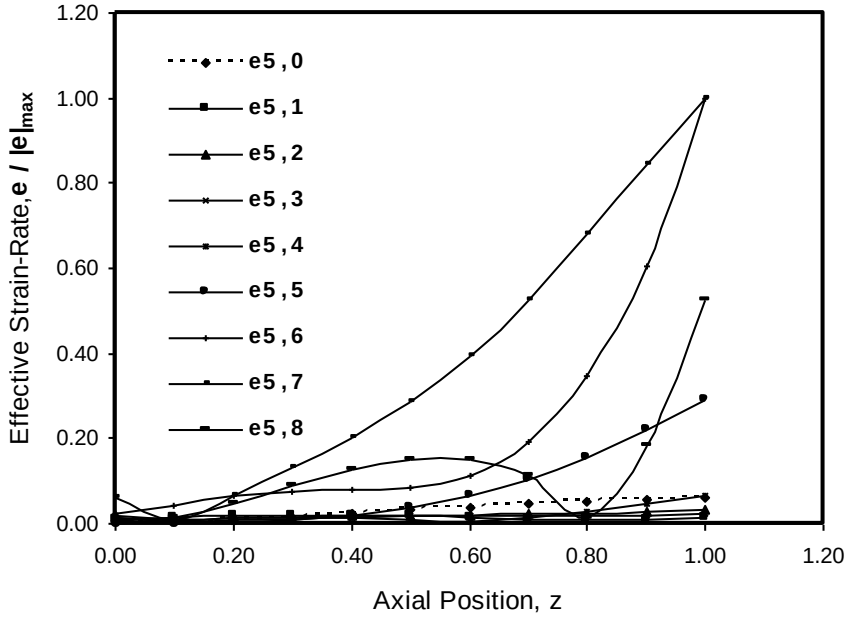

Figure 6(a): Normalised Strain-Rate Field (P = 8, N = 5, V1 = 1.0, R = 0.75, L = 1.0, m = 0.0)

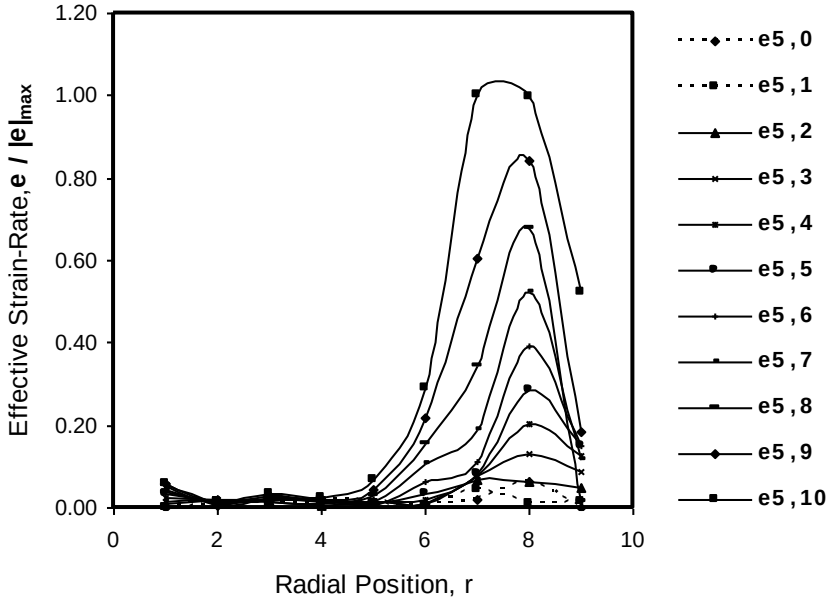

Figure 6(b): Normalised Strain-Rate Field (P = 8, N = 5, V1 = 1.0, R = 0.75, L = 1.0, m = 0.0)

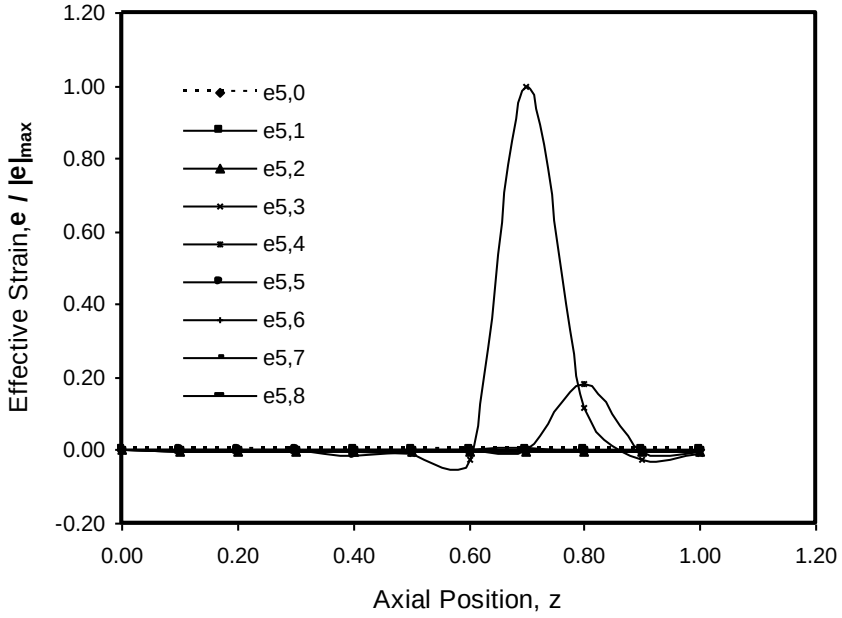

Figure 7(a): Normalised Strain Field (P = 8, N = 5, V1 = 1.0, R = 0.75, L = 1.0, m = 0.0)

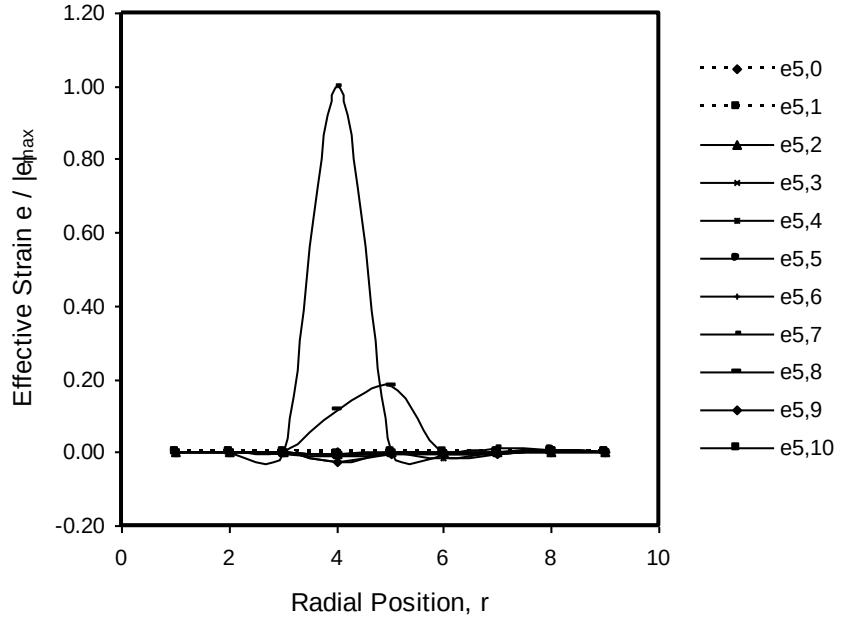

Figure 7(b): Normalised Strain Field (P = 8, N = 5, V1 = 1.0, R = 0.75, L = 1.0, m = 0.0)

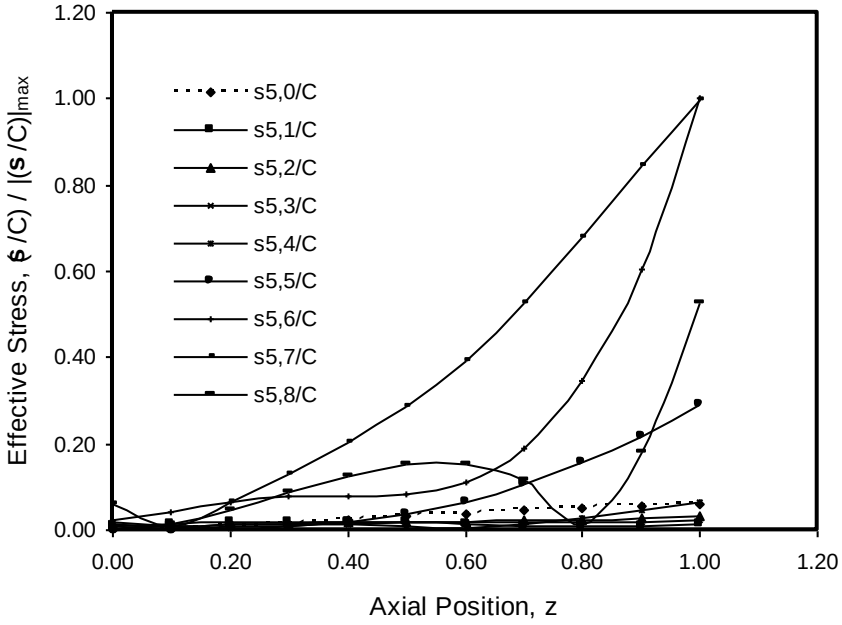

Figure 8(a): Normalised Stress Field (P = 8, N = 5, V1 = 1.0, R = 0.75, L = 1.0, m = 0.0)

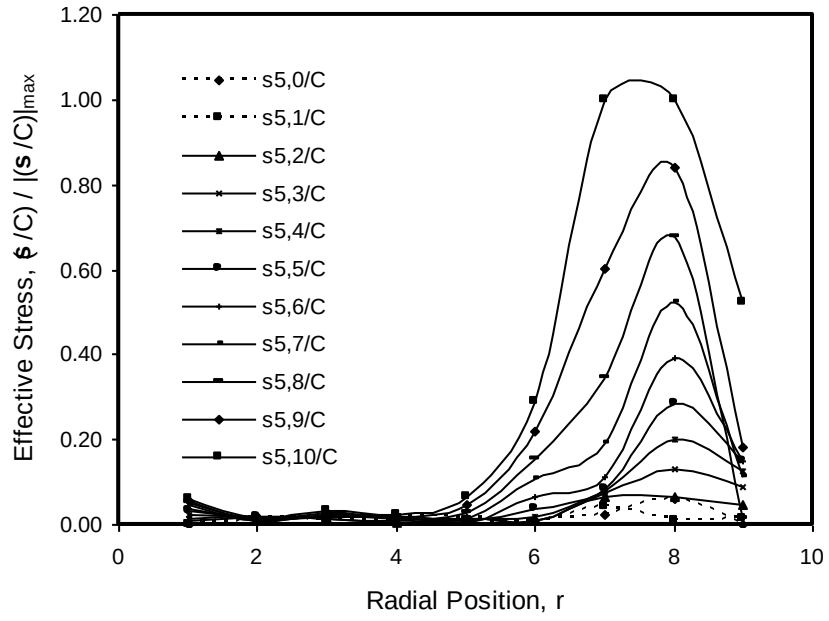

Figure 8(b): Normalised Stress Field (P = 8, N = 5, V1 = 1.0, R = 0.75, L = 1.0, m = 0.0)

The field data are found to be numerically dense, and thus, confirming the claim of Badaru [3] and Badaru et al [4], [5], [6], [7] about CNM when compared with the FDM. They are descriptive of the expected distribution of the state and flow variables as found in literature in which visioplasticity approach is used to investigate axis-symmetric metal flow in extrusion. On the other hand, the extrusion pressure (compressive stress), and the die performance parameters for the various die profiles are compared in Fig. 9. Under the considered extrusion

condition, performance of the convex circular-arc profiled die (B-C) is the worst, while that of the exponential profiled die (C-B) is the best.

Further step was also taken, in the experimentation, to verify the effects of the extrusion ratio and the interface friction factor on the performance of the dies to be able to justify the results obtained in line with those obtained using other method. The results are presented as given in Figs 10 to 12, also, for the case of extrusion through the conical die. The results showed that the extrusion pressure (compressive stress) and the die redundancy factor increased with increase in extrusion ratio. Whereas, die efficiency increased to a peak at $R_e = 1.69$, and then decreased with increase in extrusion ratio. There is no significant effect of the interface friction on these parameters except in the neighbourhood of the extrusion ratio, where the peak value of the efficiency occurred. These characteristics are quite in agreement with predictions of other methods reported in literature [7], [11], [14].

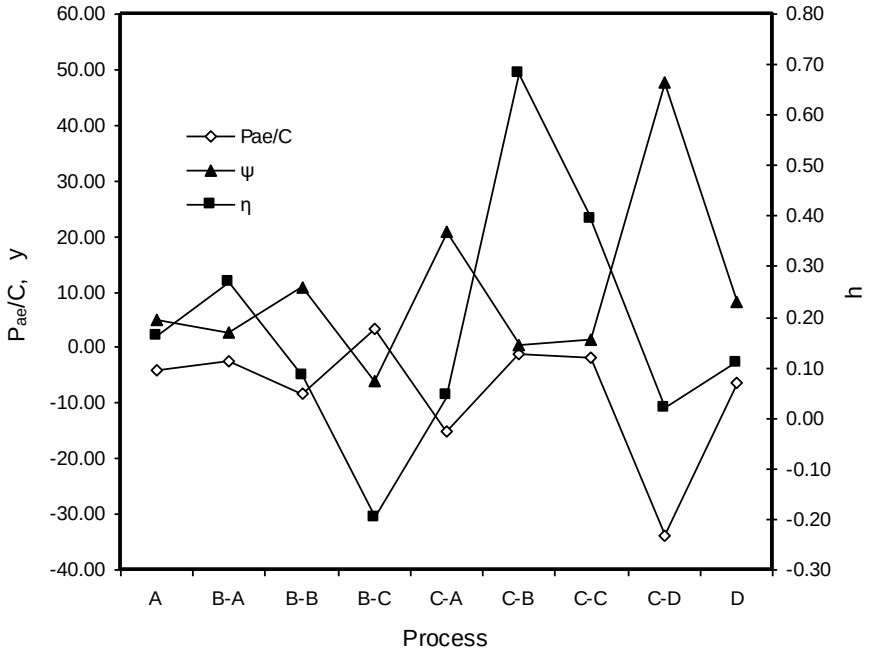

Figure 9: Comparison of the Process or Die Performance

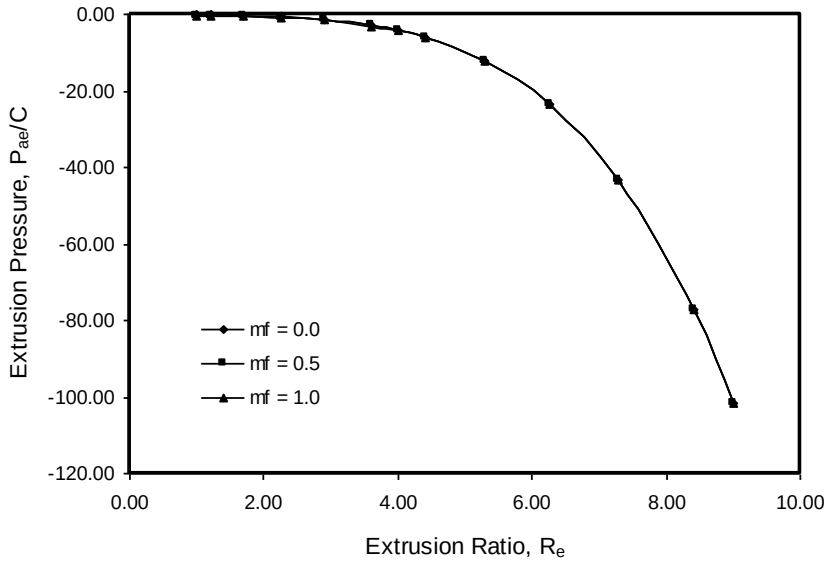

Figure 10: Variation of the Extrusion Pressure withthe Extrusion Ratio and the Interface Friction Factor

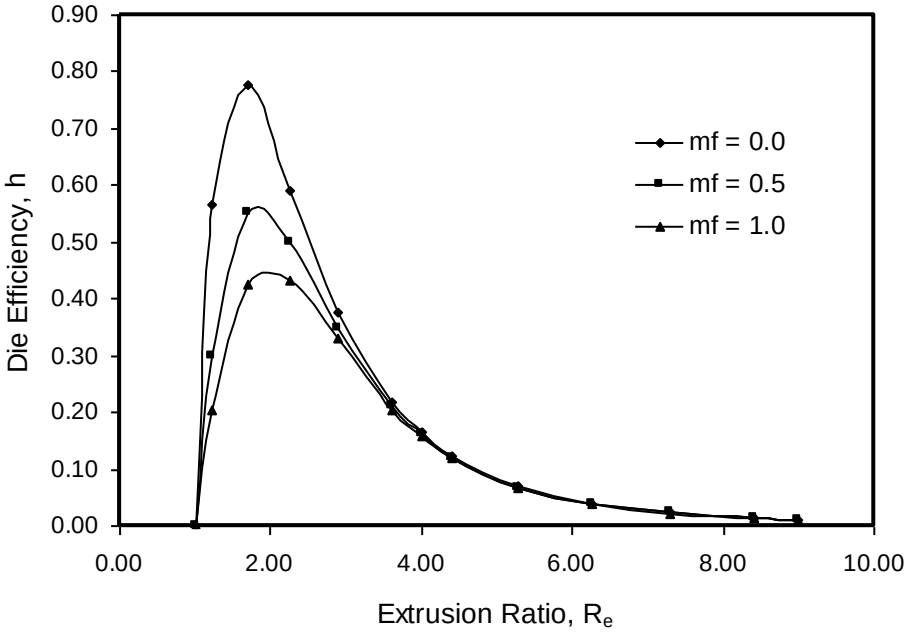

Figure 11: Variation of the Die Efficiency with the Extrusion Ratio and with the Interface Friction Factor

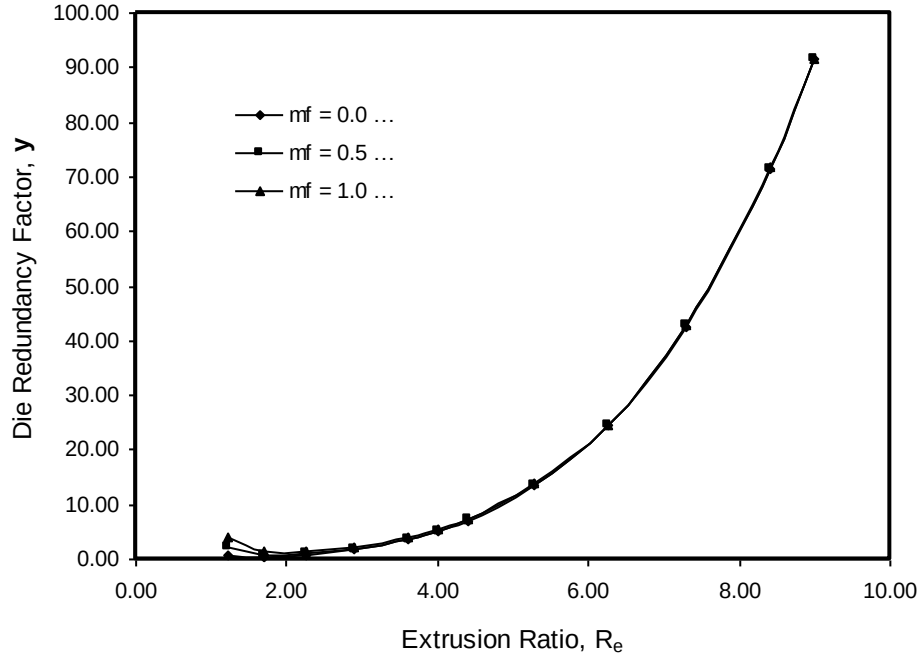

Figure 12: Variation of the Redundancy Factor with the Extrusion Ratio and the Interface Friction Factor

Application

Application of the results in extrusion process or die design is demonstrated as follows:
The obtained optimum dimensionless size for the axis-symmetric or conical die is,
$r_1 = D/d = 1.30$, $r_2 = d/d = 1.00$, $z_1 = 2l/d = 1.00$, and $z_2 = 0.00$,
These are obtained based on the dimensionless extrusion condition, $v_1 = 1.00$, $m_f = 0.00$, and $\sigma_{fp} = 0.00$. They give rise to the geometric parameters,
$L = z_1 - z_2 = z_1 = 2l/d = 1.0000$, $R_e = (r_1/r_2)^2 = (D/d)^2 = 1.6900$,
$R = (r_1^2 - r_2^2)/r_1^2 = (D^2 - d^2)/D^2 = 0.4118$, and
$\alpha = \tan^{-1}\{(r_1 - r_2)/L\} = \tan^{-1}\{(D-d)/2l\} = 16.6992^0$.
They also give rise to the process performance data,
$\eta = 0.7766$, $\psi = 0.2876$; and $P_{ae}/C = -0.3378$
The die, billet, ram, and the billet mould sizes, in dimensional terms, are afterwards derived from these specifications, using a reference billet material of UNS 50042 lead based alloy having flow stress of $\sigma_y = C = 55.08MPa$ [17], and a reference ram load of $F_r = 8.829KN\ (0.9ton)$. Thus, the billet dimensions, which result from the above specifications include,
$D_d = (2F_r/\pi P_{ae})^{1/2} = 17.4mm$, $d_b = D/r_1 = 13.4mm$, $l' = 3D_b = 52.1mm$,
$l = d_b z_1/2 = 6.7mm$, and $l_b = l' + l = 3D_b + d_b z_1/2 = 58.8mm$.
With the size of the billet known, the size of the die can be estimated. The die has been fabricated based on the estimated size, and afterwards, used to carryout extrusion operation. The results of verification experiments performed with this die are reserved for publication in another article, as space did not permit its inclusion in this paper.

Conclusion

Numerical experiments have been performed with a number of axis-symmetric profiled dies, purposely, to test the efficacy and utility of the formulated CNM technique. From the results of the solutions to direct extrusion through single-hole, symmetric dies, the following conclusions may be drawn.

1. Accuracy was found to be dependent on the combination of N and P, but no definite pattern was observed. With exception of the effective strain, the intensity of other flow variables is higher at the gridline adjacent to the friction boundary than it is at the friction and axial boundaries. It is also higher at the entrance than at the exit boundary. In terms of performance, the convex circular-arc profiled die (B-C) is the worst, while the exponential profiled die (C-B) is the best. Parametric analysis of conical die extrusion showed that the extrusion pressure and the redundancy factor increased with increase in extrusion ratio, while efficiency increased to a peak, and then decreased with increase in extrusion ratio. The interface friction has no significant effect on the performance parameters except in the neighbourhood of the extrusion ratio, where, the peak value of the efficiency occurred.
2. The method is simple and straightforward to formulate and implement, with a digital computer. It involves less complex mathematical details unlike the FEM, and possibly, BEM. It is also capable of producing dense numerical outputs unlike the FDM.
3. It is capable of providing direct and complete numerical solution of the metal flow problems in axis-symmetric extrusion together with full prediction of the process performance in any given set of conditions, just like the FDM, FEM, BEM, and visioplasticity method, and unlike the Upper bound method.
4. The assumed plastic flow zone configurations do not, geometrically, restrict its application in this respect. In the case of indirect extrusion problems, only the boundary conditions need modification in order to adapt the same formulation to the solution of the problem. Problems involving the use of square or flat faced die only require the friction boundary to be replaced with the shear boundary, as the formation of dead-metal zone may define any of the streamlined profile of the forms considered.
5. The field data obtained based on the present formulation could directly be used to obtain solutions to other axis-symmetric extrusion problems such as the asymmetric extrusion, multiple-hole extrusion, and multiple stage extrusion. However, extrusion problems involving side, Impact, lateral and rotational process may be reformulated as they may differ, considerably, in geometry from the plastic flow zone configurations considered in the present formulation.
6. It may be used to formulate steady-state shape extrusion problems, just like the plane-strain case [18], [19]. It may also be extended to analysis of other bulk metal forming problems as a way to further advance its application in the study of the mechanics of metal forming.

In its advanced stage of development, the method would be useful to the prospective designers and researchers, in industry and academics, as an alternative and very efficient numerical tool for design studies.

Acknowledgement

The authors wish to acknowledge the support of the Nigerian Defence Academy, Kaduna, Nigeria.

References

1. **Badaru**, M. A. (1998): *On Numerical Solution of Partial Differential Equations*, M.Sc Thesis (Unpublished), Department of Mathematics, University of Jos, Nigeria

2. **Badaru**, M. A. and **Onumanyi**, P. (1999): *A 4th Order Continuous Method of Lines Scheme for the Numerical Integration of Elliptic Partial Differential Equations*, NSTF (Unpublished), College of Science and Technology, Kaduna Polytechnic, Kaduna, Nigeria

3. **Badaru**, M. A. and **Oyebo**, B. A. (1999): *On Some Second –Order Off-Grid Collocation Continuous Method of Lines Scheme for the Numerical Solution of Elliptic Partial Differential Equations*, NSTF (Unpulished), College of Science and Technology, Kaduna Polytechnic, Kaduna, Nigeria
4. **Badaru**, M. A. and **Quaye**, T. O. (1998): *A formulation of the Continuous Numerical Procedure for the treatment of Equilibrium Problems in Engineering*, NECS, College of Engineering, Vol. 5, No 2, PP 412 – 419
5. **Badaru**, M. A. and **Yusuf**, Y. A. (1998): *A Continuous Method of Lines Technique for the Numerical Integration of PDES*, NSTF (Unpublished), College of Science and Technology, Kaduna Polytechnic, Kaduna, Nigeria
6. **Blazynski**, T. Z. (1993): *Metal Forming*, Manufacturing Engineer's Reference Book, Edited by Dal Koshal et al, Buterworth-Heinemann Ltd, UK: Oxford, PP 4/3 – 4/34, and 4/73 – 4/96
7. **Chakrabarty**, J. (1988): *Theory of Plasticity*, McGraw-Hill Book Company, USA: New York, PP 480 – 551
8. **Chapra**, S. C. and **Canale**, R. P. (1998): *Numerical Methods for Engineers*, 3rd Edition, McGraw-Hill, USA: New York, P 631
9. **Gurney, F. J. and De Pierre, V.** (1974): *The Influence of the Interface Condition on the Plastic Deformation Zone and the Resultant Product Integrity in Extrusion*, Journal of Engineering for Industry, Transactions of the ASME, No. 8, Vol. 96, PP 912-916
10. **Hosford**, W. F. and **Caddell**, R. M. (1983): *Metal Forming*, Prentice-Hall International, Inc. USA: Eaglewood Cliffs, New Jersey, PP 215 – 235
11. **Johnson**, W. and **Kudo**, H. (1962): *The Mechanics of Extrusion*, Manchester University Press, UK: Manchester, PP 12 – 79, and 97 – 111
12. **Lee**, Y. S. and **Male**, A. T. (1983): *Plastic Deformation Analysis of Strain-Rate Sensitive Materials under Plane-Strain Conditions*, International Journal of Mechanical Sciences, No 4, Vol. 25, PP251 – 263
13. **Lee**, Y. S. and **Patel**, M. R. (1977): *An Analysis of Plane-Strain Plastic Deformation in Metal Working Process*, Journal of Engineering for Industry, Transactions of the ASME, No8, Vol. 99, PP 727 – 732
14. **Mielnik**, E. M. (1991): *Metal-Working Science and Engineering*, MIE, McGraw-Hill Inc, USA: New York, PP 219 – 330, and 397 – 464
15. **Izelu**, C. O.; **Ebiogwu**, C. A.; and **Orumwense**, F. F. (2005): *Continuous Numerical Method in Analysis of Axis-Symmetric Extrusion Problems: Numerical Formulation*, Accepted for Publication in Academy Journal of Science and Engineering
16. **Zimerman, Z. and Avitzur, B.** (1970): *Metal Flow Through Conical Converging Dies – A Lower Upper Bound Approach Using Generalised Boundaries of the Plastic Zone*, Journal of Engineering for Industry, No. 2 Vol. 92 PP 119-129
17. **Lingaiah, L** (1994): *Machine Design Data Handbook*, McGraw-Hill, Inc, New York: USA
18. **Orumwense**, F. F., **Ebiogwu**, C. A. and **Izelu**, C. O., "On Continuous Numerical Method in Analysis of Plane-Strain Extrusion Problems, Part I: Formulation and Application", *Journal of Science and Technology Research*, Vol. 4, No. 1, 2005, PP 80-91.
19. **Orumwense**, F. F., **Ebiogwu**, C. A. and **Izelu**, C. O., "On Continuous Numerical Method in Analysis of Plane-Strain Extrusion Problems, Part II: Numerical Experiments", *Journal of Science and Technology Research*, Vol. 4, No. 2, 2005, PP 55-60.
20. **Chen, P. C. T.** (1970): *Upper Bound Solutions to Plane-Strain Extrusion Problems*, Journal of Engineering for Industry, Transactions of the ASME, No. 2, Vol. 92, PP 158-164
21. **Nagpal. V.** (1977): *Analysis of Plane-Strain Extrusion Through Arbitrarily Shaped Dies Using Flow Function*, Journal of Engineering for Industry, Transactions of the ASME, No. 8, Vol. 99, PP 754-758

22. **Chang, K. T. and Choi, J. C.** (1972): *Upper-Bound Solutions to Tube Extrusion Problems Through Curved Dies*, Journal of Engineering for Industry, Transactions of the ASME, No. 11, Vol. 94, PP 1108-1112
23. **Ishikawa, H., Hata, K. and Goto, M.** (1977): *On One Analysis of Axis-Symmetric Extrusion by the Use of Flow Lines*, Journal of Engineering for Industry, Transactions of the ASME, No. 5, Vol. 99. PP 419-423

Appendix

Extrusion Die Profile Equation

(a) Tapered or Wedge Shaped Die [20], [21]:

$$r = r(z) = r_2 + z\tan\alpha$$

(b) Parabolic Die [21]:

$$r = r(z) = r_2 + az + bz^2, \quad where, \quad a = \left\{\left(r_1 - r_2\right)/L\right\} - bL \quad and \quad b \ is \ an \ arbitrary \ coefficient$$

(c) Hyperbolic Die [20], [21]:

$$r = r(z) = \left\{r_2^2 + \left(z/L\right)^2\left(r_1^2 - r_2^2\right)\right\}^{1/2}, \quad where, \quad r_2 \le r \le r_1 \quad and \quad 0 \le z \le L$$

(d) Convex Circular-Arc Die (derived here):

$$r = r(z) = \left(r_1 + r_2\right) - \left(r_1^2 - z^2\right)^{1/2}, \quad where, \quad z = \left(r_1^2 - r_2^2\right)^{1/2}$$

Sine-Curved Die [20], [21]:

$$r = r(z) = A + B\sin\left(\pi z/2L\right), \quad where, \quad A = r_2 \quad and \quad B = r_1 - 1$$

(e) Exponential Die (derived here):

$$r = r(z) = r_1 - r_2\exp\left(-\pi z/L\right), \quad where, \ r_2 \le r \le r_1 \quad and \ 0 \le z \le L$$

(f) Concave Circular-Arc Die (derived here):

$$r = r(z) = \left\{r_2^2 + L^2 - \left(z_1 - z\right)^2\right\}^{1/2}, \quad where, \quad z_1 = z_2 + \left(r_1^2 - r_2^2\right)^{1/2}$$

(g) Elliptic Die [20], [21]:

$$r = r(z) = \left\{r_1^2 - \left[\left(L - z\right)/L\right]^2\left(r_1^2 - r_2^2\right)\right\}^{1/2}, \quad where, \ r_2 \le r \le r_1 \quad and \quad 0 \le z \le L$$

(h) Cosine-Curved Die [20], [21]:

$$r = r(z) = A - B\cos\left(\pi z/L\right), \quad where, \quad A = \frac{1}{2}\left(r_1 + r_2\right) \ and \quad B = \frac{1}{2}\left(r_1 - r_2\right)$$

GRID-LINE FLOW FUNCTIONS FOR THE CONICAL DIE EXTRUSION

$$\phi_{5,0}(z) = 0$$

$$\phi_{5,1}(z) = -0.12z + 19.27z^2 - 43.52z^3 + 38.91z^4 - 13.29z^5$$

$$\phi_{5,2}(z) = 0.27z + 40.14z^2 - 93.08z^3 + 83.21z^4 - 29.30z^5$$

$$\phi_{5,3}(z) = 0.78z + 48.70z^2 - 114.96z^3 + 99.61z^4 - 32.03z^5$$

$$\phi_{5,4}(z) = 1.59z + 41.89z^2 - 99.92z^3 + 82.76z^4 - 21.32z^5$$

$$\phi_{5,5}(z) = 2.80z + 26.25z^2 - 63.27z^3 + 63.83z^4 - 14.35z^5$$

$$\phi_{5,6}(z) = 1.02z + 42.70z^2 - 143.60z^3 + 249.02z^4 - 92.18z^5$$

$$\phi_{5,7}(z) = 22.42z - 162.00z^2 + 547.87z^3 - 818.06z^4 + 661.10z^5$$

$$\phi_{5,8}(z) = 4.00z$$